

Delayed conduction and its implications in murine *Scn5a*^{+/-} hearts: independent and interacting effects of genotype, age, and sex

Kamalan Jeevaratnam · Sui Poh Tee · Yanmin Zhang · Rebecca Rewbury ·
Laila Guzadhur · Rudolf Duehmke · Andrew A. Grace · Ming Lei ·
Christopher L.-H. Huang

Received: 1 July 2010 / Revised: 29 October 2010 / Accepted: 12 November 2010 / Published online: 3 December 2010
© The Author(s) 2010. This article is published with open access at Springerlink.com

Abstract We explored for relationships between *SCN5A* haploinsufficiency, implicated in clinical arrhythmogenicity, and right ventricular (RV) conduction disorders in Langendorff-perfused, male and female, and young (3 months) and old (>12 month old) *Scn5a*^{+/-} and wild type (WT) hearts. The investigated conditions of genotype, age, and sex affected latencies but not repolarization time courses of RV monophasic action potentials. This prompted

examination of the patterns of RV epicardial activation, its dispersion, and their interrelationships as possible arrhythmic mechanisms using a 64-channel, multi-electrode array. Mean ventricular activation times (T^*_{MEAN}), spatial dispersions (D^*_S) between recording channels/cardiac cycle, and maximum activation times (T^*_{MAX}) representing the slowest possible conduction in any given heart were all higher in old male *Scn5a*^{+/-} compared with young male and old female *Scn5a*^{+/-} and old male WT. Temporal dispersions (D^*_T) of recording channels were similarly higher in old male *Scn5a*^{+/-} compared with old male WT. All groupings of D^*_T , D^*_S , and T^*_{MAX} nevertheless linearly correlated with T^*_{MEAN} , with indistinguishable slopes. The variates explored thus influence D^*_T , D^*_S , and T^*_{MAX} through actions on T^*_{MEAN} . These findings in turn correlated with increased levels of fibrosis in young male, young female, and old male *Scn5a*^{+/-} compared with the corresponding WTs. We thus demonstrate for the first time independent and interacting effects of genotype, age, and sex on epicardial conduction and its dispersions at least partially attributable to fibrotic change, resulting in the greatest effects in old male *Scn5a*^{+/-} in an absence of alterations in repolarization time courses. This directly implicates altered depolarization in the clinical arrhythmogenicity associated with *Scn5a*^{+/-}.

K. Jeevaratnam (✉) · S. Poh Tee · Y. Zhang · R. Rewbury ·
L. Guzadhur · R. Duehmke · C. L.-H. Huang
Physiological Laboratory, University of Cambridge,
Downing Street,
Cambridge CB2 3EG, UK
e-mail: drkamalanjeeva@gmail.com

K. Jeevaratnam · L. Guzadhur · R. Duehmke · A. A. Grace ·
C. L.-H. Huang
Cardiovascular Research, Department of Biochemistry,
Hopkins Building, University of Cambridge,
Cambridge CB2 1QW, UK

M. Lei
Cardiovascular Group, School of Clinical & Laboratory Sciences,
University of Manchester Core Technology Facility (3rd floor),
University of Manchester,
Manchester M13 9NT, UK

Y. Zhang
Department of Paediatrics, First Affiliated Hospital,
Cardiovascular Ion Channel Disease Laboratory,
Xi'an Jiaotong University,
Xi'an 710061, People's Republic of China

K. Jeevaratnam
Department of Human Biology, Faculty of Medicine,
International Medical University,
Bukit Jalil,
57000, Kuala Lumpur, Malaysia

Keywords Multi-array · Biophysics · Conduction ·
Dispersion · Depolarization · Repolarization

Introduction

There has been increasing interest in the possible physiological implications of haploinsufficiencies involving

voltage-gated Na⁺ channels for clinical cardiac electrophysiological disorders. The latter include the Brugada syndrome (BrS) and progressive cardiac conduction disease (PCCD), both of which are associated with arrhythmic and conduction abnormalities [8]. Pathophysiological findings have implicated the right ventricle (RV) particularly the right ventricular outflow tract as the primary location for electrical disorders related to BrS [4]. BrS typically presents as syncope and cardiac arrest typically occurring in the third or fourth decade of life in males rather than females [14]. Thus, men with BrS have a higher prevalence of life-threatening arrhythmias than women corresponding to incidences of 9.5% and 3.8%, respectively [18]. BrS is also the leading cause of death of men under the age of 50 years in endemic regions [2]. Eighty percent of patients in Western populations and 90% in Asian countries showing clinical manifestations of BrS caused by *SCN5A* mutation are males [22]. The corresponding incidences have not been established for PCCD.

Genetically modified murine systems have been useful in exploring the consequences of *SCN5A* haploinsufficiencies. They potentially fully replicate the genetic changes associated with arrhythmogenic conditions without requiring pharmacological manipulation. Langendorff-perfused *Scn5a*^{+/-} hearts were more arrhythmic than their wild type (WT) counterparts [14, 23]. In addition, age and sex influenced murine *Scn5a*^{+/-} conduction phenotypes. *Scn5a*^{+/-} mice showed ~20% increases in the durations of their QRS complexes [17]. More recent detailed electrocardiographic (ECG) studies demonstrated independent and interacting effects of age and sex on both sino-atrial and atrioventricular function, consistent with marked conduction alterations particularly in old male *Scn5a*^{+/-} that paralleled clinical arrhythmogenic findings [7].

Electrophysiological changes in BrS have been replicated in arterially perfused canine right ventricular wedges through pharmacological manipulation. Such experiments described localized losses of the AP dome with potential arrhythmogenic effects [1, 5, 26]. RV conduction block has also been implicated in the development of arrhythmias in BrS [9, 12]. A recent human clinical trial on BrS patients attributed their type 1 ECG patterns to local depolarization as opposed to repolarization abnormalities [15]. Murine *Scn5a*^{+/-} mice similarly demonstrated prolonged ECG P wave and PR durations, right axis deviation, and second-degree AV block suggesting conduction deficiencies [14]. Their electrogram durations (EGDs) during bipolar electrogram recordings particularly following premature stimulation were also increased [23]. Both these abnormal patterns of myocardial activation and changes in EGD were attributed to re-entrant substrates resulting from altered (“fractionated”) conduction velocity distributions [19–21, 24].

The present study explores the hypothesis that *Scn5a*^{+/-} genotype, age, and sex alter cardiac conduction. This in turn would alter the dispersions in the resulting myocardial activation times at the tissue level, thereby influencing arrhythmic tendency. The electrophysiological experiments combined monophasic action potential and multi-electrode array recordings. They studied action potential properties, followed by detailed analyses of epicardial activation times and their dispersion for the first time, for subsequent comparison with morphological studies exploring for possible roles of tissue fibrosis in such changes. The observed variations in activation properties with genotype, age, and sex directly correlated with the corresponding fibrosis, suggesting a mechanism for such conduction changes. These in turn directly accounted for the previously reported clinical differences in cardiac arrhythmogenicity.

Methods

Experimental groups

Mice were housed in an animal facility at 21°C with 12-h light/dark cycles. Animals were fed sterile chow (RM3 Maintenance Diet, SDS, Witham, Essex, UK) and had free access to water. All procedures complied with the UK Home Office regulations (Animal (Scientific Procedures) Act 1986). In order to develop a comprehensive risk assessment model of the two types of mice studied, a total of 23 WT and 21 *Scn5a*^{+/-} knockout mice were used. All mice used for this study were derived from their respective 129/sv background strains to avoid any possible strain related variation in the study. The mice were divided into eight groups. Group 1 was WT male aged 3 months ($n=7$), group 2 was WT male aged >12 months ($n=5$), group 3 was WT female aged 3 months ($n=6$), group 4 was WT female aged >12 months ($n=5$), group 5 was *Scn5a*^{+/-} male aged 3 months ($n=6$), group 6 was *Scn5a*^{+/-} male aged >12 months ($n=5$), group 7 was *Scn5a*^{+/-} female aged 3 months ($n=5$), and group 8 was *Scn5a*^{+/-} female aged >12 months ($n=5$). Experiments used a Langendorff-perfused preparation adapted for the murine heart, as described previously [6, 23]. All assessments were performed fully blinded, and codes were broken only after all measurements had been performed.

Multi-electrode array recordings

A custom-made electrode array consisting of 64 separate electrodes (Teflon-coated silver wires; 0.125 mm diameter; Science Products) in an 8×8 configuration with an inter-electrode distance of 0.55 mm was used. Unipolar recordings were performed by placing the multi-electrode array on the right epicardium with the reference electrode, acting as

the indifferent pole at the base of the heart. The 64 recording electrodes were connected through shielded wires to two 32-channel amplifiers (SCXI-1102 C, National Instruments Corporation (U.K.) Ltd, Newbury, UK). Sampling frequency for each signal was set at 1 kHz. The signals were continuously stored on disk and displayed on screen using a custom-developed program, written in Labview 7.0 (National Instruments Corporation (U.K.) Ltd, Newbury, UK).

For the off-line analysis, signals were displayed on screen in sets of eight to 16 electrograms. The activation time was determined as the point of maximal negative slope and marked with a cursor. After marking all significant waveforms in all leads, the activation times were then displayed in a grid representing the layout of the original recording array. All activation times, in milliseconds, were related to the timing of the first detected waveform. Activation maps were drawn using Microsoft Office Excel 2007 (Microsoft Corporation, Silicon Valley, USA).

Monophasic action potential recordings

A bipolar platinum stimulating electrode (1-mm interpolar spacing) was placed on the interventricular septum, and a monophasic action potential (MAP) recording electrode (Hugo Sachs, Harvard Apparatus) was placed on the corresponding right epicardium. During this time, MAPs showed stable baselines, rapid upstroke phases that reached consistent amplitudes, and smooth repolarization phases, all of which are known to be characteristic of high-fidelity MAP recordings. MAPs were amplified, band-pass filtered (0.5 Hz–1 kHz: Neurolog NL104 Amplifier, NL125/6 Filter; Digitimer, Welwyn Garden City, Herts, UK) and digitized at a sampling frequency of 5 kHz (micro1401, Cambridge Electronic Design, Cambridge, UK). Hearts were paced at a cycle length of 125 ms. Analysis of MAPs was performed using Spike II software (Cambridge Electronic Design).

Quantification of cardiac fibrosis

Isolated hearts were flushed with Krebs buffer and perfused with 4% buffered formalin for 5 min before being immersed in formalin overnight. After fixation, gross transverse sections were cut from base to apex, and the hearts were subjected to routine tissue processing and paraffin embedding. Paraffin sections of 7 μm thickness were then cut and stained with Sirius red stain (Sigma-Aldrich, Dorset, UK). All sections were subsequently viewed, magnified, and digitally acquired using the Nano Zoomer 2.0 Digital Pathology system (Hamamatsu, Hertfordshire, UK). For the quantification of fibrosis, two randomly selected photomicrographs with a minimum distance of 14 μm from each other were taken for every heart.

Following a $\times 2$ magnification, a custom-made 17 cm \times 23 cm morphometric grid, consisting of square boxes of dimension 1 cm \times 1 cm, corresponding to a 0.26 mm \times 0.26 mm area of tissue, was then superimposed on each photomicrograph. Only squares occupied either completely or partially by cardiac tissues were counted. Similarly, squares containing fibrotic changes were then counted, and this was expressed as a percentage of the total cardiac tissue area. An average percentage of fibrotic changes for every heart taken from the two photomicrographs were obtained and then accumulated for every group to provide the mean percentage of fibrotic tissue.

Statistical analysis

Comparisons where appropriate were performed by analysis of variance or *t* test with SPSS software (SPSS UK, Woking, Surrey, UK). Regression coefficients were calculated by $t = r\sqrt{(n-2)/\sqrt{(1-r^2)}}$, with $n-2$ degrees of freedom [16]. Statistical significance was assumed at $P < 0.05$, $P < 0.01$, or $P < 0.001$ where applicable.

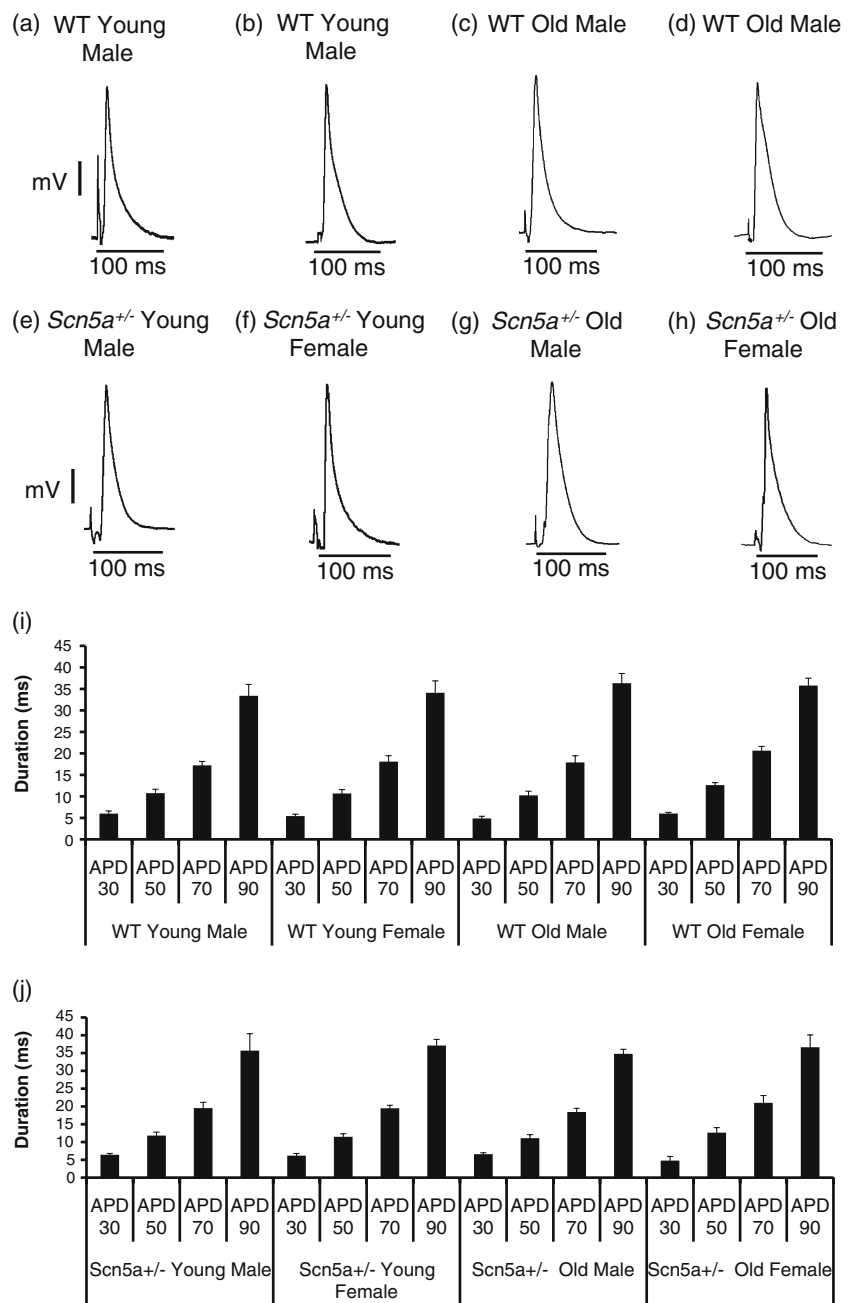
Results

MAP assessments of action potential repolarization and latencies

The initial MAP studies observed alterations in action potential latencies that prompted the more detailed studies of such latencies that followed. Thus, Fig. 1a–h shows typical action potential waveforms including their latencies from each of the experimental groups. Figure 1i, j quantifies the resulting measures of action potential duration (APD), obtained at 30%–90% full repolarization, in the eight experimental groups. APD₃₀, APD₅₀, APD₇₀, and APD₉₀ values (Fig. 1i, j) showed no statistical differences between experimental groups in tests for either independent or interacting stratifications by genotype, age, or sex.

In contrast, significant differences were observed concerning the MAP latencies (Table 1). Thus, the initial stratifications simply by genotype demonstrated that *Scn5a*^{+/-} hearts had significantly longer ($P < 0.001$) latencies compared with WT hearts. Stratifications by genotype and age then demonstrated that there were no latency differences between young and old WT but longer latencies ($P = 0.002$) in old *Scn5a*^{+/-} when compared with young *Scn5a*^{+/-}. Both young and old *Scn5a*^{+/-} showed longer ($P = 0.029$; $P = 0.001$) latencies compared with young and old WT, respectively. A third stratification assessed for independent effects of genotype and sex. This confirmed an absence of latency differences between male and female WT. However, latency

Fig. 1 Mean repolarization durations represented by values of APD₃₀, APD₅₀, APD₇₀, and APD₉₀ for WT and *Scn5a*^{+/-} hearts sorted by age and sex. APDs were obtained from Langendorff-perfused hearts isolated from healthy mice. Representative MAPs waveform recordings are shown for all the eight experimental groups (a–h). Durations of APDs for the stratification by genotype only, genotype and age, and genotype and sex are not shown. The full stratification of both WT and *Scn5a*^{+/-} mice by both age and sex is represented by i and j, respectively. All APD values were not significantly different irrespective of genotype, age, or sex through all stratification levels



was longer ($P=0.032$) in male *Scn5a*^{+/-} compared with female *Scn5a*^{+/-}. Male *Scn5a*^{+/-} showed longer ($P<0.001$) latencies compared with male WT; differences were absent in the corresponding females.

The final stratification examined for the interacting effects of genotype, age, and sex. Both old male *Scn5a*^{+/-} and old female *Scn5a*^{+/-} hearts showed longer ($P=0.044$; $P=0.046$) latencies compared with the young male *Scn5a*^{+/-} and young female *Scn5a*^{+/-} hearts, respectively. Such differences were absent in the WT population. Furthermore, young male *Scn5a*^{+/-} and old male *Scn5a*^{+/-} had longer ($P=0.006$; $P=0.004$) latencies compared with young male WT and old

male WT, respectively. All other comparisons were not significantly different. Together, these findings suggest that MAP latencies were influenced by independent and interacting effects of genotype, age, and sex. These findings prompted the more detailed multi-array studies that follow.

Multi-array analysis for conduction and its dispersion

Figure 2 shows representative waveforms obtained using a 64-channel multi-electrode array placed on the right ventricles of Langendorff-perfused, intrinsically beating hearts. The records were obtained from two rows, marked

Table 1 Latency (ms) in monophasic action potential activation

Animal	Samples	Average \pm SE
WT (total)	27	15.66 \pm 0.77 a
WT young	14	14.79 \pm 0.54 b
WT old	13	16.60 \pm 1.49 c
WT male	14	16.36 \pm 1.09 d
WT female	13	14.91 \pm 1.01
WT young male	6	15.71 \pm 0.64 e
WT young female	8	14.10 \pm 0.76
WT old male	8	16.84 \pm 1.88 f
WT old female	5	16.22 \pm 2.67
<i>Scn5a</i> ^{+/-} (total)	21	21.20 \pm 1.11 a
<i>Scn5a</i> ^{+/-} young	11	17.85 \pm 1.36 b, g
<i>Scn5a</i> ^{+/-} old	10	24.25 \pm 1.10 c, g
<i>Scn5a</i> ^{+/-} male	11	23.41 \pm 1.17 d, h
<i>Scn5a</i> ^{+/-} female	10	18.77 \pm 1.67 h
<i>Scn5a</i> ^{+/-} young male	4	20.10 \pm 1.23 e, i
<i>Scn5a</i> ^{+/-} young female	6	16.15 \pm 1.88 j
<i>Scn5a</i> ^{+/-} old male	7	25.14 \pm 1.35 f, i
<i>Scn5a</i> ^{+/-} old female	4	22.70 \pm 1.88 j

Means with similar lowercase letters differ significantly from each other at $P < 0.05$

1–8 and 9–16, respectively, in the array from (a) old male WT, (b) old male *Scn5a*^{+/-}, (c) old female WT, and (d) old female *Scn5a*^{+/-} hearts. Most of the recording elements indicated a presence of electrical activity reflecting effective contact with the apposed tissue. This took the form of similar biphasic waveforms with different latencies. It was therefore possible to characterize each trace by a single activation time during offline analysis for all 64 channels. Such latencies were measured by locating a cursor to the

point of maximal negative slope in the trace. This was repeated in five consecutive beats in all hearts that were studied. The resulting activation times obtained were then displayed in a matrix representing the layout of the original recording array through the use of a false color code in which the time of earliest to latest activation were represented by red and a gradual color change to green.

Figure 3 exemplifies the resulting activation maps in five successive cardiac cycles from typical young (a, b, e, and f) and old (c, d, g, and h), male (a, e, c, and g), female (b, f, d, and h), WT (a, b, c, and d), and *Scn5a*^{+/-} hearts (e, f, g, and h). Most of the activation maps obtained from the WT hearts showed a general pattern of sequential activation in which one region of the matrix appeared to be activated first, and this was then followed by a successive spread of activation through the remainder of the area from which recordings were made. This would be compatible with either a spread of excitation within the plane of the epicardium or an orderly arrival of activation from the endocardium to the epicardium. However the *Scn5a*^{+/-} hearts often did not show this orderly pattern and often exhibited a more random excitation of different channels. Rather than describing our results solely in terms of a sequential activation within the plane of the epicardium, we therefore adopted a more empirical description quantifying the activation times, their spatial and temporal dispersions, and their maximum values.

Figure 3e–h thus indicates that the *Scn5a*^{+/-} hearts showed a greater frequency of areas reflecting late activation times in comparison with WT. This trend was more prominent in males compared with females and was particularly marked in the old male *Scn5a*^{+/-} (Fig. 3g) hearts whether compared with remaining groups of either *Scn5a*^{+/-} or WT hearts. In contrast, among the WT hearts

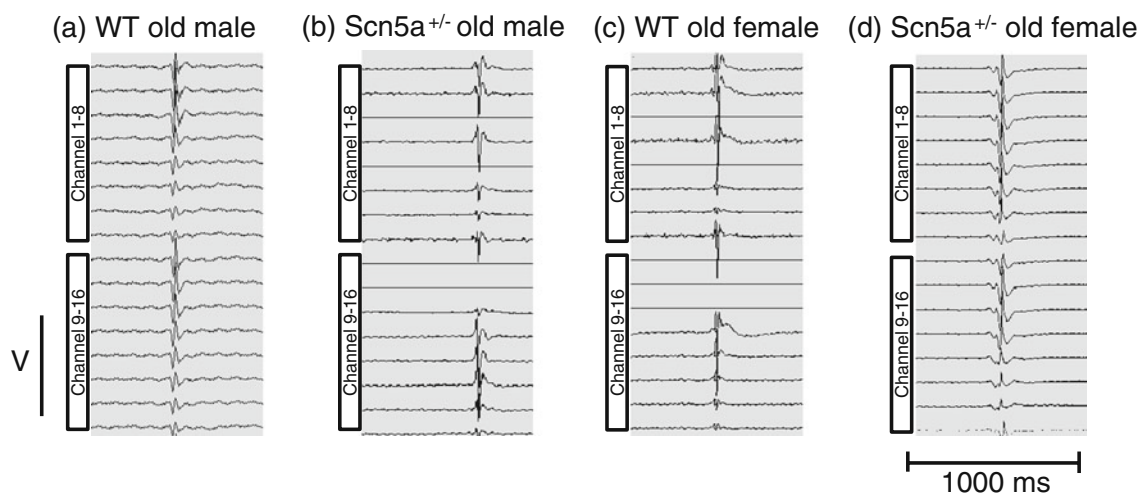


Fig. 2 Representative biphasic waveform recordings. Representative recordings of 16 channels obtained from a 64-channel multi-electrode array from: WT old male (a), *Scn5a*^{+/-} old male (b), WT old female

(c), and *Scn5a*^{+/-} old female (d). Most recording channels showed a presence of electrical activity during measurements from intrinsically beating Langendorff-perfused hearts

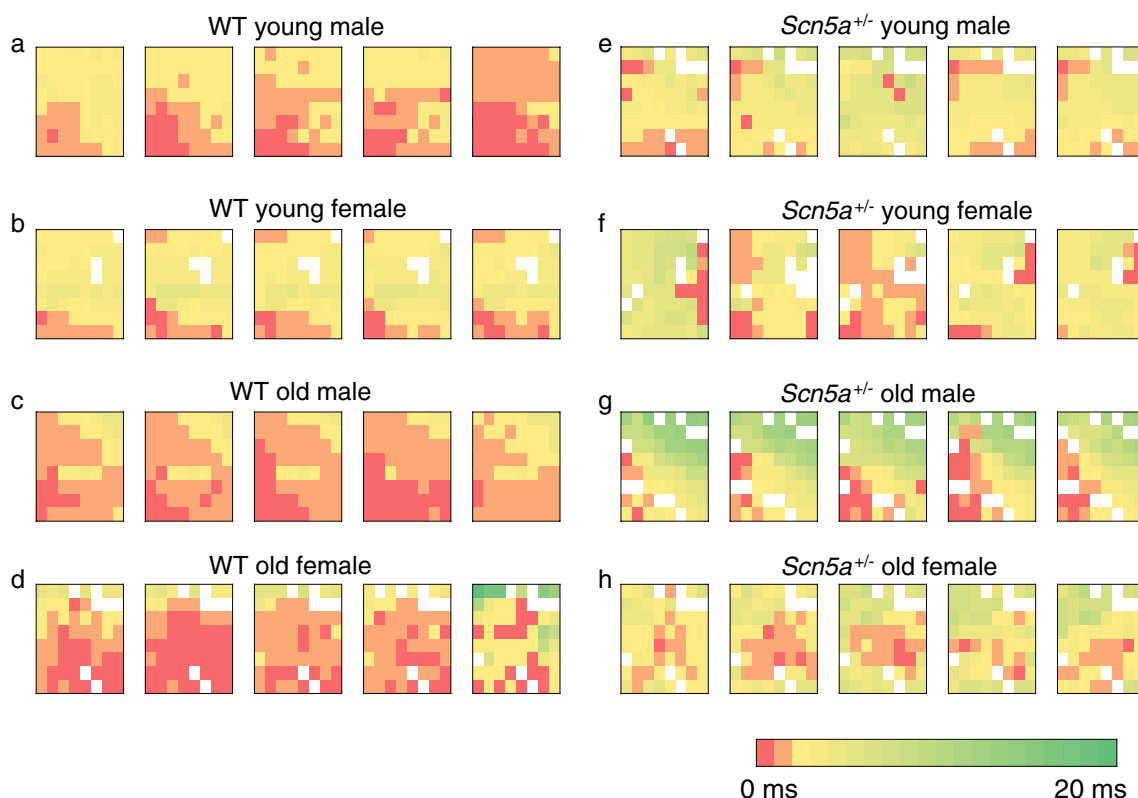


Fig. 3 Representative activation maps of five successive cardiac cycles in WT and *Scn5a*^{+/-} hearts grouped by age and sex. The study population was stratified into: WT young male (**a**), WT young female (**b**), WT old male (**c**), WT old female (**d**), *Scn5a*^{+/-} young male (**e**), *Scn5a*^{+/-} young female (**f**), *Scn5a*^{+/-} old male (**g**), and *Scn5a*^{+/-} old female (**h**). Recordings using a 64-channel multi-electrode array on intrinsically beating Langendorff-perfused mouse hearts were per-

formed. Activation times for 64 channels were determined in five successive cardiac cycles in all hearts to produce the respective activation maps. Color gradients represent the various activation time for every channel. Time of first activation is represented as *red* followed by gradual color change to *green* representing time of last activation

(Fig. 3a–d), the old female WT (Fig. 3d) appeared to have the most delayed activation time compared with the other WT groups, although this distinction was not as clear as for the *Scn5a*^{+/-}. These findings suggest a greater propensity to delayed activation times in *Scn5a*^{+/-} in comparison with WT. They further suggest that the interacting influences of age, sex, and genotype, with older male *Scn5a*^{+/-} show particularly longer delays. These observations were subsequently quantified through determinations of the following parameters. All these involved a collection of multi-array data over five consecutive cardiac cycles, i.e., over a time span of 1 s.

Mean activation times

Firstly, a *mean activation time*, T_{MEAN} , was used to describe the overall activation time within any given heart. This was obtained from the activation times in all channels averaged over five beats. These values were then used to obtain average values, T^*_{MEAN} , for each group of hearts investigated. Table 2 summarizes the resulting T^*_{MEAN}

values, expressed as means \pm standard errors of the mean from the different levels of stratification of the experimental population. Such successive stratifications demonstrated significant independent and interacting effects of genotype, age, and sex.

Thus, initial comparison of the population as a whole by genotype prior to the subsequent stratifications involving age and sex demonstrated that T^*_{MEAN} was significantly higher ($P=0.046$) in the *Scn5a*^{+/-} hearts when compared with WT hearts. Stratification of the dataset by both genotype and age yielded four groups: young WT, old WT, young *Scn5a*^{+/-} and old *Scn5a*^{+/-}. The resulting comparisons showed that there were no significant differences in T^*_{MEAN} , between any of these groups. Stratifications by both genotype and sex gave contrasting groups consisting of male WT, female WT, male *Scn5a*^{+/-} and female *Scn5a*^{+/-}. Values of T^*_{MEAN} between male and female WT were then indistinguishable. However, they were significantly higher ($P=0.047$) in male *Scn5a*^{+/-} hearts compared with female *Scn5a*^{+/-} hearts. They were also significantly higher ($P=0.042$) for male *Scn5a*^{+/-} compared

Table 2 T^*_{MEAN} (ms) values in right ventricular murine hearts

Animal	Samples	Average \pm SE
WT (total)	23	2.45 \pm 0.25 a
WT young	13	2.29 \pm 0.20
WT old	10	2.65 \pm 0.52
WT male	12	2.22 \pm 0.37 b
WT female	11	2.71 \pm 0.33
WT young male	7	2.30 \pm 0.28
WT young female	6	2.29 \pm 0.32
WT old male	5	2.09 \pm 0.85 c
WT old female	5	3.21 \pm 0.57
<i>Scn5a</i> ^{+/-} (total)	21	3.37 \pm 0.38 a
<i>Scn5a</i> ^{+/-} young	11	2.92 \pm 0.45
<i>Scn5a</i> ^{+/-} old	10	3.87 \pm 0.62
<i>Scn5a</i> ^{+/-} male	11	4.08 \pm 0.63 b, d
<i>Scn5a</i> ^{+/-} female	10	2.59 \pm 0.24 d
<i>Scn5a</i> ^{+/-} young male	6	2.84 \pm 0.81 e
<i>Scn5a</i> ^{+/-} young female	5	3.02 \pm 0.31
<i>Scn5a</i> ^{+/-} old male	5	5.58 \pm 0.42 c, e, f
<i>Scn5a</i> ^{+/-} old female	5	2.17 \pm 0.27 f

Means with similar lowercase letters differ significantly from each other at $P < 0.05$

with the male WT hearts. However, such a distinction was not observed between female *Scn5a*^{+/-} and female WT.

The final level of stratification additionally resolved interacting effects between the variables of genotype, age, and sex. This gave the groups: young male WT, old male WT, young female WT, old female WT, young male *Scn5a*^{+/-}, old male *Scn5a*^{+/-}, young female *Scn5a*^{+/-}, and old female *Scn5a*^{+/-}. This showed that regardless of age and sex, there were no statistical differences observed in T^*_{MEAN} among the four groups of WT hearts. However, T^*_{MEAN} showed a more diverse pattern of statistical significances within the *Scn5a*^{+/-} group. T^*_{MEAN} in the old male *Scn5a*^{+/-} was significantly higher whether compared with the old female *Scn5a*^{+/-} ($P = 0.009$), the young male *Scn5a*^{+/-} ($P = 0.021$), as well as the old male WT ($P = 0.028$). Thus T^*_{MEAN} was greater in the old male *Scn5a*^{+/-} hearts than in any of the remaining groups. In contrast, it was statistically identical between young male *Scn5a*^{+/-} and young female *Scn5a*^{+/-}, old female *Scn5a*^{+/-}, and young female *Scn5a*^{+/-} as well as between old female *Scn5a*^{+/-} and old female WT.

Temporal dispersions of activation times

Secondly, a *temporal dispersion of activation times*, D_T was derived to describe the variation in activation time at a given channel again averaged through five successive cardiac cycles. The standard deviation of the activation

times, T_{MEAN} , defined above, measured from each channel, was determined from five successive cardiac cycles. Readings from each of the 64 individual channels in the array were then averaged. This yielded the temporal dispersion D_T for the heart under study. These values were then used to obtain average values, D^*_T , for each group of hearts investigated.

Table 3 summarizes the resulting D^*_T values from the different levels of stratification. Stratification by genotype alone showed that D^*_T was higher in the *Scn5a*^{+/-} hearts compared with the WT hearts ($P = 0.048$). However, stratifications of the study population by both genotype and age demonstrated that D^*_T was indistinguishable whether between young and old animals within a given genotype or between WT and *Scn5a*^{+/-} within a given age group. Stratifications by genotype and sex similarly revealed that values of D^*_T showed no significant differences between male WT and female WT and between male *Scn5a*^{+/-} and female *Scn5a*^{+/-}. However, values of D^*_T were significantly higher ($P = 0.028$) in the male *Scn5a*^{+/-} mice compared with the male WT mice. The final level of stratification separating interacting effects between genotype, age, and sex showed that there were no statistical differences in D^*_T between the four groups of WT hearts. These similarities were also observed within the groups of *Scn5a*^{+/-} hearts. However, D^*_T was significantly higher ($P = 0.046$) in old male *Scn5a*^{+/-} compared with old male WT.

Table 3 D^*_T (ms) values in right ventricular murine hearts

Animal	Samples	Average \pm SE
WT (total)	23	0.88 \pm 0.11 a
WT young	13	0.79 \pm 0.10
WT old	10	1.01 \pm 0.21
WT male	12	0.78 \pm 0.12 b
WT female	11	1.00 \pm 0.19
WT young male	7	0.82 \pm 0.11
WT young female	6	0.75 \pm 0.20
WT old male	5	0.72 \pm 0.24 c
WT old female	5	1.29 \pm 0.31
<i>Scn5a</i> ^{+/-} (total)	21	1.24 \pm 0.14 a
<i>Scn5a</i> ^{+/-} young	11	1.08 \pm 0.15
<i>Scn5a</i> ^{+/-} old	10	1.43 \pm 0.25
<i>Scn5a</i> ^{+/-} male	11	1.41 \pm 0.25 b
<i>Scn5a</i> ^{+/-} female	10	1.07 \pm 0.12
<i>Scn5a</i> ^{+/-} young male	6	1.07 \pm 0.27
<i>Scn5a</i> ^{+/-} young female	5	1.09 \pm 0.15
<i>Scn5a</i> ^{+/-} old male	5	1.82 \pm 0.40 c
<i>Scn5a</i> ^{+/-} old female	5	1.03 \pm 0.20

Means with similar lowercase letters differ significantly from each other at $P < 0.05$

Spatial dispersions of activation times

Thirdly a *spatial dispersion*, D_S , was obtained to describe the dispersion of activation times between recording channels in a given cardiac cycle averaged through five successive cycles. Activation times were obtained for each of the 64 channels in any given cycle. The standard deviation of these was then calculated. Averaged values of this standard deviation were then obtained from five consecutive cardiac cycles to derive D_S . These values were then used to obtain average values, D^*_S , for each group of hearts investigated.

Table 4 summarizes such D^*_S values following stratification into WT and $Scn5a^{+/-}$ hearts and then demonstrated no differences in D^*_S . Further stratification of the dataset by genotype and age demonstrated no significant differences in D^*_S regardless of genotype or age. Similarly, stratifications by genotype and sex showed no significant differences in D^*_S between any pair of experimental groups. Nevertheless, the final level of stratification resolved interacting effects between genotype, age, and sex. There were then no statistical differences observed in D^*_S between the four groups of WT hearts. However, D^*_S appeared to show a more diverse pattern of statistical significances within the $Scn5a^{+/-}$ group. Thus, it was significantly higher in the old male $Scn5a^{+/-}$ compared with the young male $Scn5a^{+/-}$ ($P=0.045$), the old female

$Scn5a^{+/-}$ ($P=0.009$), as well as the old male WT. Thus, D^*_S was greater in the old male $Scn5a^{+/-}$ hearts than in any of the remaining groups. In contrast, D^*_S was indistinguishable between young male $Scn5a^{+/-}$ and young female $Scn5a^{+/-}$, old female $Scn5a^{+/-}$ and young female $Scn5a^{+/-}$, as well as between old female $Scn5a^{+/-}$ and old female WT.

Maximum activation times

Finally, a *maximum activation time*, T_{MAX} , provided a simple measure of the slowest possible conduction that could take place in any given heart. It was determined by measuring the activation time from the channel showing the greatest delay in electrical activation through all five cardiac cycles from which data were collected. Such data from all the hearts in any given group were used to obtain an average, T^*_{MAX} .

Table 5 summarizes these T^*_{MAX} values, obtained from the different levels of stratification of the experimental groups. Hearts were also sorted by individual T_{MAX} values falling in the respective ranges of 0–3, 4–6, 7–10, and >10 ms, in order to emphasize groups showing either the greatest or smallest extremes in such values. These successive stratifications demonstrated significant independent and interacting effects of genotype, age, and sex. Thus, even the simple initial, genotypic, comparison of the population as a whole demonstrated significantly higher ($P=0.002$) T^*_{MAX} values in the $Scn5a^{+/-}$ compared with the WT. $Scn5a^{+/-}$ and WT correspondingly showed distributions biased toward greater and smaller T_{MAX} values, respectively.

Further stratification of the dataset by both genotype and age demonstrated different effects of age within each genotype. Thus, there were statistically indistinguishable and similarly distributed T^*_{MAX} values in old WT and young WT hearts. However, such T^*_{MAX} values were significantly greater ($P=0.031$) in old $Scn5a^{+/-}$ than young $Scn5a^{+/-}$, reflecting distributions skewed in old $Scn5a^{+/-}$ towards higher values, >10 ms, of T_{MAX} . In contrast, analysis of the effects of genotype within each age group demonstrated significantly higher ($P=0.046$) T^*_{MAX} values in the young $Scn5a^{+/-}$ hearts compared with the young WT. Similarly, T^*_{MAX} values were significantly higher ($P=0.016$) in the old $Scn5a^{+/-}$ compared with old WT.

Stratifications by both genotype and sex revealed that there were no differences attributable to sex within each genotype. Thus, T^*_{MAX} values were similar both between male and female WT and between male and female $Scn5a^{+/-}$. However, comparisons of the effects of genotype within each sex group showed significantly higher ($P=0.007$) T^*_{MAX} values in the male $Scn5a^{+/-}$ than the male WT. In contrast, T^*_{MAX} values were statistically indistinguishable between female WT and female $Scn5a^{+/-}$.

Table 4 D^*_S (ms) values in right ventricular murine hearts

Animal	Samples	Average \pm SE
WT (total)	23	1.61 \pm 0.18
WT young	13	1.51 \pm 0.21
WT old	10	1.74 \pm 0.32
WT male	12	1.55 \pm 0.29
WT female	11	1.68 \pm 0.21
WT young male	7	1.65 \pm 0.31
WT young female	6	1.35 \pm 0.28
WT old male	5	1.41 \pm 0.59 a
WT old female	5	2.07 \pm 0.22
$Scn5a^{+/-}$ (total)	21	1.99 \pm 0.24
$Scn5a^{+/-}$ young	11	1.57 \pm 0.25
$Scn5a^{+/-}$ old	10	2.46 \pm 0.36
$Scn5a^{+/-}$ male	11	2.40 \pm 0.40
$Scn5a^{+/-}$ female	10	1.55 \pm 0.14
$Scn5a^{+/-}$ young male	6	1.52 \pm 0.47 b
$Scn5a^{+/-}$ young female	5	1.62 \pm 0.13
$Scn5a^{+/-}$ old male	5	3.44 \pm 0.24 a, b, c
$Scn5a^{+/-}$ old female	5	1.48 \pm 0.27 c

Means with similar lowercase letters differ significantly from each other at $P<0.05$

Table 5 T^*_{MAX} (ms) and frequencies of hearts with different ranges of T_{MAX} values

Animal	Samples	Average \pm SE	Intervals			
			0–3 ms	4–6 ms	7–10 ms	>10 ms
WT (total)	23	5.87 \pm 0.65 a	8	6	8	1
WT young	13	5.31 \pm 0.73 b	5	4	4	0
WT old	10	6.60 \pm 1.17 c	3	2	4	1
WT male	12	5.33 \pm 1.03 d	5	4	2	1
WT female	11	6.46 \pm 0.79	3	2	6	0
WT young male	7	5.29 \pm 0.99	2	3	2	0
WT young female	6	5.33 \pm 1.17	3	1	2	0
WT old male	5	5.40 \pm 2.21 e	3	1	0	1
WT old female	5	7.80 \pm 0.74	0	1	4	0
<i>Scn5a</i> ^{+/-} (total)	21	9.29 \pm 0.86 a	0	6	9	6
<i>Scn5a</i> ^{+/-} young	11	7.46 \pm 0.62 b, f	0	4	6	1
<i>Scn5a</i> ^{+/-} old	10	11.30 \pm 1.44 c, f	0	2	3	5
<i>Scn5a</i> ^{+/-} male	11	10.46 \pm 1.48 d	0	3	2	6
<i>Scn5a</i> ^{+/-} female	10	8.00 \pm 0.62	0	3	7	0
<i>Scn5a</i> ^{+/-} young male	6	6.83 \pm 1.01 g	0	3	2	1
<i>Scn5a</i> ^{+/-} young female	5	8.20 \pm 0.58	0	1	4	0
<i>Scn5a</i> ^{+/-} old male	5	14.80 \pm 1.36 e, g, h	0	0	0	5
<i>Scn5a</i> ^{+/-} old female	5	7.80 \pm 1.16 h	0	2	3	0

Means with similar lowercase letters differ significantly from each other at $P < 0.05$

The final level of stratification additionally resolved interacting effects between the variables of genotype, age and sex. Firstly, it considered the effects of age and sex within any given genotypic group. This importantly demonstrated that age and sex exerted no effects upon T^*_{MAX} within all four WT groups of animals. Thus, T^*_{MAX} values were statistically indistinguishable between all four WT groups. In contrast, age and sex exerted marked effects upon T^*_{MAX} among the four *Scn5a*^{+/-} groups of animals. The most striking finding was that the old male *Scn5a*^{+/-} showed the highest T^*_{MAX} compared with all the other groups. An analysis of differences attributable to age in sex-matched *Scn5a*^{+/-} showed that T^*_{MAX} values were significantly higher ($P = 0.006$) in the old male *Scn5a*^{+/-} than in the young male *Scn5a*^{+/-}. However, such values were similar in the old female *Scn5a*^{+/-} compared with the young female *Scn5a*^{+/-}. Analysis of differences attributable to sex in age-matched *Scn5a*^{+/-} showed that T^*_{MAX} values were significantly higher ($P = 0.008$) in old male *Scn5a*^{+/-} compared with old female *Scn5a*^{+/-}. This was in contrast to indistinguishable T^*_{MAX} values in the young male *Scn5a*^{+/-} and young female *Scn5a*^{+/-}.

Secondly, it considered the effects of genotype on animals matched by both age and sex. This demonstrated that T^*_{MAX} values were significantly higher ($P = 0.034$) in old male *Scn5a*^{+/-} than old male WT. This finding was also reflected in the distributions. Thus, all the *Scn5a*^{+/-} old male hearts had a T_{MAX} value of >10 ms in comparison

with the rest of the group. In contrast, there were no other significant differences in T^*_{MAX} values among the remaining groups.

Correlations between activation times and measures of their dispersion

The above results demonstrate significant interacting effects of age, sex, and genotype upon measures of activation times, T^*_{MEAN} , its dispersions, as represented by D^*_{T} , D^*_{S} , and T^*_{MAX} . Thus, in the group as a whole, genotype exerted significant effects upon T^*_{MEAN} , D^*_{T} , and T^*_{MAX} . Stratification by genotype and age influenced only the T^*_{MAX} values and that by genotype and sex influenced T^*_{MEAN} , D^*_{T} , and T^*_{MAX} . The final stratifications revealed effects on all four variables. All significant changes tended to occur in the same direction, consistent with causal relationships between them. Furthermore, significant changes in D^*_{T} and D^*_{S} were always accompanied by corresponding changes in T^*_{MEAN} , but the reverse was not always the case. Together, these findings suggest a trend toward increased dispersions of activation with increasing activation time, establishing the latter variant as a major determinant of such dispersion. These features prompted us to explore for quantitative relationships between the measures of dispersion with their corresponding T^*_{MEAN} .

Firstly, we accordingly compared D^*_{T} , D^*_{S} , and T^*_{MAX} values from each individual heart against their corresponding T^*_{MEAN} . Figure 4 exemplifies the resulting

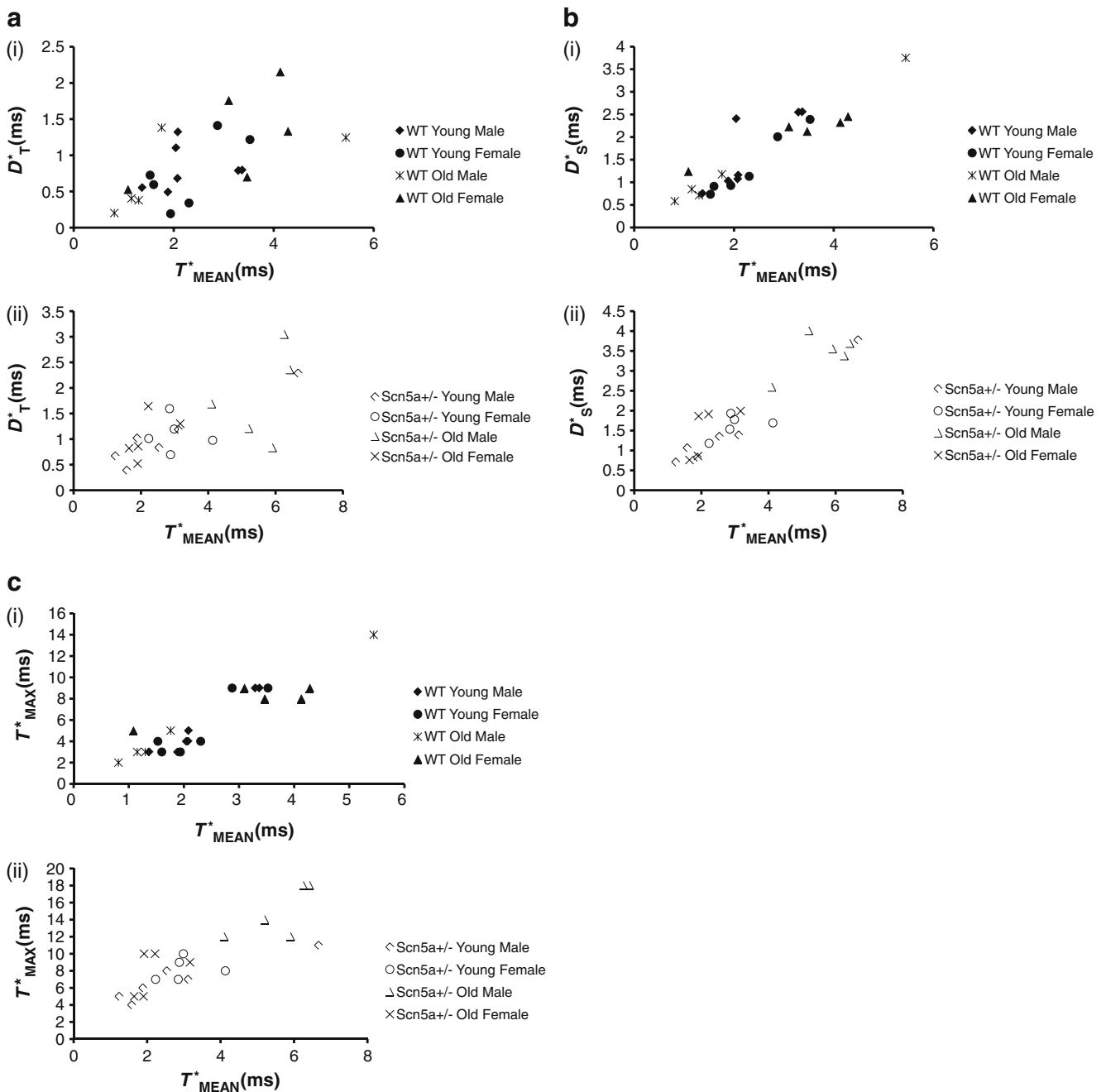


Fig. 4 Representative plots summarizing linear correlation and regression analysis of D^*_T , D^*_S , and T^*_{MAX} against T^*_{MEAN} . Plots for D^*_T (a), D^*_S (b), and T^*_{MAX} (c) for WT (i) and $Scn5a^{+/-}$ (ii). The regression analysis demonstrated significant correlations between the

plots of D^*_T (a), D^*_S (b), and T^*_{MAX} (c) against T^*_{MEAN} when these were sorted by the WT (i) and $Scn5a^{+/-}$ (ii) genotypes. The analysis then went on to explore such correlations when the experimental groups were instead sorted by age and sex. In all six resulting cases, these demonstrated significant correlations between the measures of dispersion and the mean activation time. Thus, Table 6 summarizes the results of correlations of the n available

parameters of D^*_T , D^*_S , and T^*_{MAX} on the ordinate and T^*_{MEAN} on the abscissa with slopes that were not significantly different whether following stratification by genotype, age, or sex

values of D^*_T , D^*_S , and T^*_{MAX} with T^*_{MEAN} following sorting of the data by genotype (WT, $Scn5a^{+/-}$), age (young and old), and sex (male and female). All the regression coefficients, r^2 , demonstrated significant correlations with T^*_{MEAN} .

Secondly, having established that T^*_{MEAN} significantly influences D^*_T , D^*_S , and T^*_{MAX} in all groups analyzed, we examined if such influences may vary with genotype, age,

Table 6 Results of linear correlation analysis of D^*_T , D^*_S , and T^*_{MAX} against T^*_{MEAN} showing values of correlation coefficient, r^2 , t values of its significance and values of slope, m

	Samples	df	D^*_T			D^*_S			T^*_{MAX}		
			r^2	t	m	r^2	t	m	r^2	t	m
WT	23	21	0.36	3.45 ^a	0.26±0.08	0.83	10.28 ^b	0.70±0.12	0.85	10.96 ^b	1.97±0.46
<i>Scn5a</i> ^{+/-}	21	19	0.48	4.16 ^b	0.28±0.08	0.87	11.24 ^b	0.45±0.11	0.59	5.21 ^b	2.71±0.30
Young	24	22	0.49	4.64 ^b	0.21±0.09	0.74	7.95 ^b	0.63±0.16	0.54	5.11 ^b	0.92±0.45
Old	20	18	0.43	3.65 ^a	0.34±0.05	0.89	12.24 ^b	0.52±0.10	0.81	8.67 ^b	2.76±0.26
Male	23	21	0.57	5.32 ^b	0.24±0.07	0.89	13.1 ^b	0.63±0.12	0.87	11.85 ^b	2.42±0.14
Female	21	19	0.33	3.07 ^a	0.53±0.15	0.62	5.54 ^b	0.31±0.09	0.21	2.24 ^c	2.26±0.61

Populations were sorted by genotype, age, and sex
 df degrees of freedom

^a $P < 0.01$, significant correlations deduced from values of t

^b $P < 0.001$, significant correlations deduced from values of t

^c $P < 0.05$, significant correlations deduced from values of t

and sex. Values of the slope for each regression line, m , were obtained and analyzed. As demonstrated by Table 6, m values were statistically indistinguishable between WT and *Scn5a*^{+/-}, between young and old and between male and female. Thus, in contrast to activation time, each of these factors (i.e., genotype, age, and sex) is unlikely to make major determinants by themselves to the degree of dispersion. Thus, in the present study, the major determinant for dispersion appears to be activation time.

Quantitative evaluation of cardiac fibrosis

The present study quantitatively demonstrated major differences in electrophysiological conduction characteristics as a result of the interacting effects of age, sex, and genotype for the first time. These findings agreed with recent qualitative histological evidence that the *Scn5a*^{+/-} mutation interacts with age in producing microscopic myocardial fibrotic changes [10, 17]. The present experiments therefore proceeded to make quantitative histological explorations for effects of genotype, age, and sex upon such fibrotic change. It was then possible to assess the extent to which these might correlate with the corresponding conduction properties.

Figure 5 exemplifies typical histological sections from young (a, b, e, and f) and old (c, d, g, and h), male and (a, e, c, and g) female (b, f, d, and h), and WT (a, b, c, and d) and *Scn5a*^{+/-} hearts (e, f, g, and h). Table 7 summarizes the results of morphometric assessments of the percentage of fibrotic tissue using a stratification scheme for the experimental groups identical to that adopted for the electrophysiological results. The initial stratification by genotype demonstrated a significantly ($P < 0.001$) greater proportion of fibrotic tissue in the *Scn5a*^{+/-} than the WT hearts. The second level of stratification by genotype and age demonstrated more fibrosis

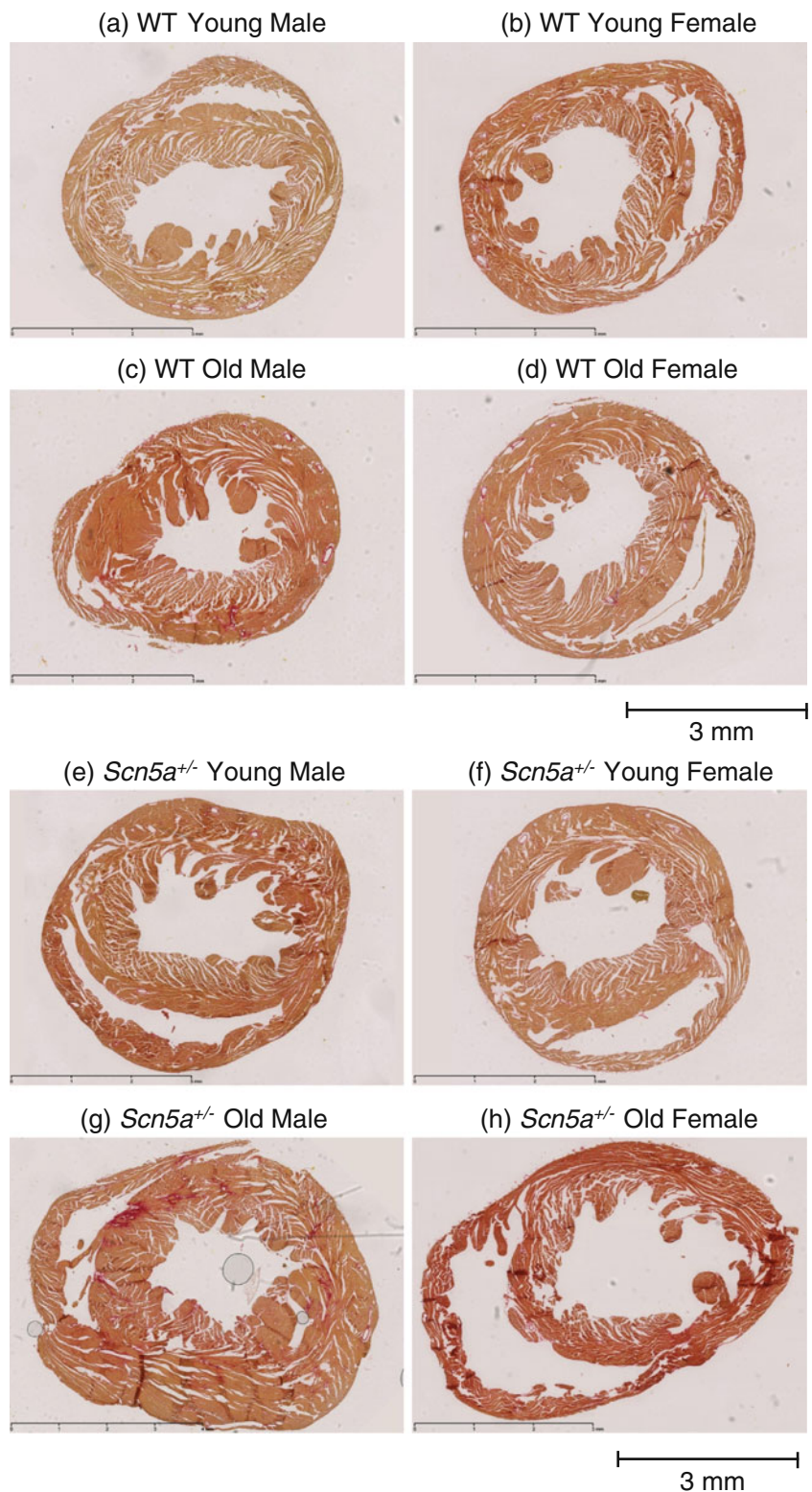
in old WT and old *Scn5a*^{+/-} hearts ($P < 0.001$ and $P = 0.013$, respectively) than their young counterparts within the same genotypic groups. Comparisons across genotype similarly demonstrated more fibrosis in the young and old *Scn5a*^{+/-} compared with the young and old WT ($P < 0.001$ and $P = 0.002$ respectively).

The third level of stratification by genotype and sex additionally demonstrated effects of sex on levels of fibrosis but only in the *Scn5a*^{+/-} hearts. There was more ($P = 0.013$) fibrosis in male compared with female *Scn5a*^{+/-}, but no such differences between male and female WT. Comparisons across genotype revealed greater fibrosis ($P < 0.001$) in the male *Scn5a*^{+/-} compared with male WT. Such differences were absent between female *Scn5a*^{+/-} and WT. The final level of stratification by genotype, age, and sex similarly corresponded closely to the electrophysiological results. Thus, within genotypic groups, there was more fibrosis in the old male *Scn5a*^{+/-} than either the young male *Scn5a*^{+/-} or the old female *Scn5a*^{+/-} ($P < 0.001$ and $P < 0.001$ respectively). There was more fibrosis in the old male WT than the young male WT ($P = 0.006$) but not the old female WT ($P > 0.05$). Comparisons across genotypic group demonstrated more fibrosis in young male *Scn5a*^{+/-}, young female *Scn5a*^{+/-} and old male *Scn5a*^{+/-} compared with the young male WT, young female WT, and old male WT ($P = 0.001$, $P = 0.002$, and $P < 0.001$, respectively). Such differences were not observed between the old female *Scn5a*^{+/-} hearts and old female WT hearts.

Discussion

The present studies complement our previous reports on the electrophysiological consequences of *Scn5a* haploinsufficiency

Fig. 5 Representative slide for cardiac fibrosis staining in WT and *Scn5a*^{+/-} hearts grouped by age and sex. The study population was stratified into: WT young male (a), WT young female (b), WT old male (c), WT old female (d), *Scn5a*^{+/-} young male (e), *Scn5a*^{+/-} young female (f), *Scn5a*^{+/-} old male (g), and *Scn5a*^{+/-} old female (h). Hearts were routinely stained with Sirius red, and morphometric analysis for percentage of fibrosis was performed for all eight groups. Areas of increased red uptake signify presence of fibrotic changes. Horizontal bar below sections in each panel denotes a 3 mm distance



in genetically modified murine systems. These reported increased arrhythmogenic tendencies [14] that were accompanied by increases in electrogram durations during extracellular recording studies in murine *Scn5a*^{+/-} hearts [23]. These were

followed by *in vivo* studies that followed cohorts of *Scn5a*^{+/-} mice stratified by the severity of their conduction changes defined using 18–22- and >22-ms cutoffs in their QRS durations, in parallel with similar clinical stratifications shown

Table 7 Percentage of fibrotic tissue in murine hearts

Animal	Samples	Average \pm SE
WT	23	4.73 \pm 0.80 a
WT young	13	2.18 \pm 0.26 b, c
WT old	10	7.27 \pm 1.08 b, d
WT male	12	4.50 \pm 1.02 e
WT female	11	4.95 \pm 1.27
WT young male	7	2.22 \pm 0.41 f, g
WT young female	6	2.12 \pm 0.33 h
WT old male	5	7.93 \pm 0.95 f, i
WT old female	5	6.84 \pm 1.75
<i>Scn5a</i> ^{+/-}	21	14.38 \pm 2.06 a
<i>Scn5a</i> ^{+/-} young	11	9.26 \pm 0.93 c, j
<i>Scn5a</i> ^{+/-} old	10	18.92 \pm 3.14 d, j
<i>Scn5a</i> ^{+/-} male	11	18.42 \pm 2.82 e, k
<i>Scn5a</i> ^{+/-} female	10	8.60 \pm 1.00 k
<i>Scn5a</i> ^{+/-} young male	6	8.78 \pm 1.40 g, l
<i>Scn5a</i> ^{+/-} young female	5	9.74 \pm 1.37 h
<i>Scn5a</i> ^{+/-} old male	5	24.84 \pm 1.53 i, l, m
<i>Scn5a</i> ^{+/-} old female	5	7.08 \pm 1.08 m

Means with similar lowercase letters differ significantly from each other at $P < 0.05$

by BrS patients containing *SCN5A* mutations [10]. These demonstrated parallel changes in conduction and in semi-quantitative measures of fibrosis that varied with age, confirming previous correlations between increased PR intervals and age specifically in the *Scn5a*^{+/-} [17]. Our subsequent study using closely similar sample numbers then described conduction velocity alterations associated with increased cardiac fibrosis and down-regulation of connexin expression in old *Scn5a*^{+/-} mice. We thus demonstrated that such alterations in conduction velocity were not solely dependent on reduced *Scn5a* expression. We then however did not stratify for the interacting effects of age and sex [25]. Finally, recent ECG measurements particularly of PR and RR intervals then went on to fully clarify both the independent and the interacting effects of genotype, age, and sex upon conduction characteristics in fully stratified experimental groups. These showed in particular that old male *Scn5a*^{+/-} showed marked increases in such conduction durations [7].

We proceeded to examine mean conduction and its dispersion at the tissue, rather than the ECG level, using multi-array recording methods, comparing these with MAP assessments of action potential waveform durations and latencies. Our multi-electrode array studies were less extensive (550 vs 300 μm ; 64 vs 247 channels; 1- vs 2–4-kHz sampling) than those used previously [25]. These findings were then correlated with differences in levels of fibrosis, though they did not explore for changes in connexin and Na^+ channel expression. Nevertheless, they

complemented our earlier studies in exploring for interacting effects of genotype, age, and sex and permitted a novel statistical analysis of activation times and their dispersions both over the regions of interest studied and through successive intrinsic beats. Stratification of these results into experimental groups paralleled and therefore permitted direct comparisons with the earlier, similarly stratified, ECG results [7], thus adding to these a full clarification of alterations in electrogram latencies at the tissue level. They went further to achieve direct correlations of such altered conduction with quantitative assessments of the level of fibrosis. The latter suggested possible mechanisms for such conduction changes, thereby extending and complementing earlier findings that had also assessed for possible existence of fibrosis [10, 17].

The present experiments accordingly provided a more detailed analysis of these conduction disorders on a more microscopic scale as reflected in the activation times shown by epicardial excitation during multi-electrode array recording. They systematically examined the effects of genotype, age, and sex, corresponding to eight experimental groups, on cardiac conduction, determined how these effects alter the subsequent dispersions, and related these findings to morphometric analysis of fibrosis to test this as a possible mechanism underlying such electrophysiological changes.

Initially, the time course of monophasic action potential recovery was assessed at 30%, 50%, 70%, and 90% recovery. This yielded similar values through the stratifications indicated above, suggesting a similarity in all their recovery characteristics. A recent report [11] had described right epicardial APDs in *Scn5a*^{+/-} that differed from WT. However, this only considered a single age of mouse between 4 and 8 months. It did not perform further stratifications by sex, in contrast to the present study. This difference in findings between 3 and ~6 months suggests that APD can vary with age. Such a notion would parallel recent descriptions of atrial remodeling phenomena in the presence of *Scn5a* modification [6] and merits further investigation. Nevertheless, the present findings do demonstrate differing action potential latencies corroborating earlier ECG findings [7] under circumstances in which action potential characteristics remained similar.

Our initial qualitative assessment of activation maps derived from activation times at each channel demonstrated that the *Scn5a*^{+/-} group generally showed higher activation times compared with WT, particularly the older males. They also showed a more heterogenous pattern of activation, at times with multiple random firing points. Such random activation suggests that the spread of electrical activity in the right ventricle is fragmented, conceivably reflecting patterns of spread suggested on recent occasions [3]. In this respect, it would resemble recent reports describing fragmented QRS complexes characteristics in

BrS patients [13]. It further suggests the presence of areas within the right ventricle that depolarize later than the rest particularly in the *Scn5a*^{+/-} mice. Such a finding is compatible with the late potentials, which have previously been observed in signal-averaged ECG thought to represent regions undergoing delayed depolarization than the remaining ventricular tissue [27]. Other clinical studies have previously identified the presence of similarly heterogeneous patterns in BrS patients [9].

In this study, rather than suggesting a sequential spread of conduction within the plane of the epicardium, the *Scn5a*^{+/-} mice suggested an irregular pattern of activation in which each epicardial site was separately activated by a radial propagation of excitation through the myocardium. These patterns would be compatible with a greater likelihood of re-entrant events between neighboring epicardial sites and thereby result in arrhythmic substrate. This would be particularly the case if neighboring sites showed strongly different activation times. These might be detectable through the maximum activation times observed and might even then serve as an arrhythmic trigger in parallel with the arrhythmogenicity observed in the corresponding clinical conditions. Quantitative assessments compared such patterns in terms of overall activation times and their dispersions, for the first time. These in turn demonstrated differences that were attributable to both independent and interacting effects of genotype, age, and sex.

Firstly, a *mean activation time* (T^*_{MEAN}) provided an overall representation of epicardial activation properties resulting from myocardial conduction. This was significantly higher in the *Scn5a*^{+/-} compared with WT hearts. However, such differences were less clear with further stratification by both genotype and age. Nevertheless, stratification by both genotype and sex resulted in higher T^*_{MEAN} values in *Scn5a*^{+/-} male compared with *Scn5a*^{+/-} female hearts. This established an interacting effect of genotype and sex on conduction disorders in mutation carriers. Thus, sex affects T^*_{MEAN} values only in the mutant and not in the WT. The final stratification involving genotype, age, and sex further established interacting effects on T^*_{MEAN} values particularly within the *Scn5a*^{+/-} group. Taken together, this analysis demonstrated that alterations in T^*_{MEAN} values, likely reflecting altered conduction, are a major feature of *Scn5a*^{+/-} hearts particularly in old male hearts. They also demonstrated that the earlier electrocardiographic findings [7], suggestive of alterations in overall conduction, further extended to the pattern of epicardium activation. Such a finding in the murine *Scn5a*^{+/-} model reflects recent clinical findings implicating conduction disorder as feature in arrhythmogenic BrS patients [15].

Secondly, a *temporal dispersion* D^*_T described the temporal variation in activation time at epicardial sites between cardiac cycles. D^*_T values were significantly

higher in the *Scn5a*^{+/-} hearts. Although stratifications by genotype and age did not yield significant differences, those by genotype and sex revealed difference between male *Scn5a*^{+/-} and male WT. Finally, stratification by all three variates revealed differences between old male *Scn5a*^{+/-} and old male WT. Taken together, such findings suggest that where an influence occurs, temporal dispersions of the ventricular activation time are primarily affected by genotype and not by age and sex.

Thirdly, a *spatial dispersion* (D^*_S) described the spatial variation in activation time of the different epicardial sites in a single cardiac cycle. Unlike both T^*_{MEAN} and D^*_T , values for D^*_S were indistinguishable when stratified by genotype, genotype and age, and genotype and sex. However, the final stratification by genotype, age, and sex yielded distinct significances. Thus, it demonstrated that the old male *Scn5a*^{+/-} hearts had higher dispersions than not only the old male WT but also the other *Scn5a*^{+/-} groups. Such a finding suggests that differences in dispersions of activation times arise only following interacting influences involving all three variates.

Fourthly, the *maximum activation time* (T^*_{MAX}) described the features of those epicardial sites showing the greatest activation delays that might potentially actually trigger arrhythmia as suggested above. T^*_{MAX} values were significantly higher in the *Scn5a*^{+/-} compared with WT hearts, thus establishing an independent effect of genotype on this value. Stratification by genotype and age showed marked effects. They revealed higher T^*_{MAX} values in young *Scn5a*^{+/-} than young WT, in old *Scn5a*^{+/-} than old WT, and in old *Scn5a*^{+/-} than young *Scn5a*^{+/-}. Stratification by genotype and sex revealed higher T^*_{MAX} values in male *Scn5a*^{+/-} than male WT. Finally, stratification by all three variates revealed strongly interacting effects specifically in the *Scn5a*^{+/-} and not the WT. This resulted in higher T^*_{MAX} values in old male *Scn5a*^{+/-} compared with old male WT, old female *Scn5a*^{+/-}, and young male *Scn5a*^{+/-}.

The D^*_T , D^*_S , and T^*_{MAX} findings thus suggested significant differences in dispersions of epicardial activation times between particular experimental groups. The final analysis assessed the extent to which these differences could be attributed to variations in conduction as represented by T^*_{MEAN} . This would extend the electrocardiographic observations in our previous paper [7] with the physiological findings at the tissue level described here. Such a notion would be compatible with our statistical observations in which significant changes in D^*_T and D^*_S were always accompanied by corresponding changes in T^*_{MEAN} , but with the reverse not being always the case. Accordingly, we explored for correlations between the above measures of dispersion with such activation times. This demonstrated linear correlations between each of the variables, D^*_T , D^*_S , and T^*_{MAX} upon T^*_{MEAN} . Each gave

statistically significant linear correlations whether the experimental populations were sorted by genotype, age, or sex. Furthermore, this yielded statistically indistinguishable slopes, suggesting that these correlations were similar through all these conditions. This analysis is thus compatible with a situation in which conduction properties form the major determinant for these dispersions, regardless of genotype, age, and sex.

A final series of investigations tested a hypothesis that implicated the degree of fibrosis in the conduction properties found in each experimental group. They complemented previous qualitative reports that had not fully assessed effects of both age and sex in connection with fibrotic changes associated with the *Scn5a*^{+/-} mutation [10, 17]. The *Scn5a*^{+/-} hearts then showed generally greater fibrosis than WT hearts. Furthermore, even young *Scn5a*^{+/-} mice showed increased fibrosis relative to the corresponding young WT. However, this predisposition appeared to apply only to the male and not the female *Scn5a*^{+/-} mice. Consequently, old male *Scn5a*^{+/-} showed greater fibrosis than the young male *Scn5a*^{+/-}, the old female *Scn5a*^{+/-}, and the old male WT hearts. The quantitative morphometric analysis of collagen staining used here thus demonstrated patterns of fibrosis that closely matched the electrophysiological findings among the experimental groups sorted by genotype, age, and sex.

In summary, we have investigated for independent and interacting effects of the *Scn5a*^{+/-} genotype, age, and sex on epicardial activation and its dispersion in murine hearts, which have been previously used to model the corresponding human clinical conditions. Our findings show that genotype, age, and sex all exert independent and interacting effects on cardiac conduction with the greatest effects on ventricular activation times in the old male *Scn5a*^{+/-}. Such changes directly correlated with the corresponding levels of fibrosis, thereby directly implicating fibrotic changes as important participants in these conduction differences. These effects took place despite an absence of corresponding differences in action potential recovery times as reflected in action potential durations measured at 30%, 50%, 70%, and 90% full recovery. These effects on conduction correlated with greater dispersions of activation times in the *Scn5a*^{+/-} hearts as a whole compared with WT. The involved variations in activation time are both between cardiac cycles at any given recording site and between recording sites within a given cardiac cycle, as well as the maximum activation times that were obtained during such recordings. These dispersions have been implicated in arrhythmic substrate, as assessed by electrogram analysis in clinical studies [19]. In murine *Scn5a*^{+/-}, the increased EGD that had been reported previously [23] are directly comparable with the increased dispersion in epicardial activation reported here. This finding again was

particularly marked in hearts from old male *Scn5a*^{+/-} mice. The subsequent regression analysis gave regression coefficients that attributed each of these dispersions directly to differences in conduction. In each case, there was dependence between variates, *m*, that was similar through all the stratifications that the experiments explored. Such findings implicate similar actions of genotype, age, or sex upon each dispersion, which are mediated through actions on the conduction process. Together, these findings also demonstrate that in contrast to their similar epicardial repolarization features, conduction and dispersion, which are features of depolarization, are prominent in the murine *Scn5a*^{+/-} model, particularly in older males. They may thus contribute to the reported arrhythmogenic properties of this system.

Acknowledgements Kamalan Jeevaratnam is supported by the Maxis Scholarship for Excellence Program, funded and administered by Maxis Communications Berhad (Malaysia). He is also the recipient of the Cambridge Commonwealth Trust Bursary Award and the Lundgren Research Award. Rebecca Rewbury was supported by a Wellcome Trust Summer Research Studentship. This research is funded by the British Heart Foundation, the Medical Research Council, and the Wellcome Trust, United Kingdom. We thank Prof. Wim Lammers of the Faculty of Medicine, UAE University, for help in the design and conception of the multi-array unit and to Downing College and the Avrith Grant for conference support.

Open Access This article is distributed under the terms of the Creative Commons Attribution Noncommercial License which permits any noncommercial use, distribution, and reproduction in any medium, provided the original author(s) and source are credited.

References

1. Alings M, Wilde A (1999) “Brugada” syndrome: clinical data and suggested pathophysiological mechanism. *Circulation* 99:666–673
2. Antzelevitch C (2002) Brugada syndrome: historical perspectives and observations. *Eur Heart J* 23:676–678
3. Caldwell BJ, Trew ML, Sands GB, Hooks DA, LeGrice IJ, Smail BH (2009) Three distinct directions of intramural activation reveal nonuniform side-to-side electrical coupling of ventricular myocytes. *Circ Arrhythm Electrophysiol* 2:433–440
4. Capulzini L, Brugada P, Brugada J, Brugada R (2010) Arrhythmia and right heart disease: from genetic basis to clinical practice. *Rev Esp Cardiol* 63:963–983
5. Gussak I, Antzelevitch C, Bjerregaard P, Towbin JA, Chaitman BR (1999) The Brugada syndrome: clinical, electrophysiologic and genetic aspects. *J Am Coll Cardiol* 33:5–15
6. Guzhur L, Pearcey SM, Duehmke RM, Jeevaratnam K, Hohmann AF, Zhang Y, Grace AA, Lei M, Huang CL (2010) Atrial arrhythmogenicity in aged *Scn5a*^{+/-}/*DeltaKPQ* mice modeling long QT type 3 syndrome and its relationship to Na⁺ channel expression and cardiac conduction. *Pflugers Arch* 460:593–601
7. Jeevaratnam K, Zhang Y, Guzhur L, Duehmke RM, Lei M, Grace AA, Huang CL (2010) Differences in sino-atrial and atrio-ventricular function with age and sex attributable to the *Scn5a*^{+/-} mutation in a murine cardiac model. *Acta Physiol Oxf* 200:23–33
8. Kyndt F, Probst V, Potet F, Demolombe S, Chevallier JC, Baro I, Moisan JP, Boisseau P, Schott JJ, Escande D, Le Marec H (2001)

- Novel SCN5A mutation leading either to isolated cardiac conduction defect or Brugada syndrome in a large French family. *Circulation* 104:3081–3086
9. Lambiase PD, Ahmed AK, Ciaccio EJ, Brugada R, Lizotte E, Chaubey S, Ben-Simon R, Chow AW, Lowe MD, McKenna WJ (2009) High-density substrate mapping in Brugada syndrome: combined role of conduction and repolarization heterogeneities in arrhythmogenesis. *Circulation* 120(106–17):1–4
 10. Leoni AL, Gavillet B, Rougier JS, Marionneau C, Probst V, Le Scouarnec S, Schott JJ, Demolombe S, Bruneval P, Huang CL, Colledge WH, Grace AA, Le Marec H, Wilde AA, Mohler PJ, Escande D, Abriel H, Charpentier F (2010) Variable Na(v)1.5 protein expression from the wild-type allele correlates with the penetrance of cardiac conduction disease in the Scn5a(+/-) mouse model. *PLoS ONE* 5:e9298
 11. Martin CA, Zhang Y, Grace AA, Huang CL (2010) Increased right ventricular repolarization gradients promote arrhythmogenesis in a murine model of Brugada syndrome. *J Cardiovasc Electrophysiol* 21:1153–1159
 12. Meregalli PG, Wilde AA, Tan HL (2005) Pathophysiological mechanisms of Brugada syndrome: depolarization disorder, repolarization disorder, or more? *Cardiovasc Res* 67:367–378
 13. Morita H, Kusano KF, Miura D, Nagase S, Nakamura K, Morita ST, Ohe T, Zipes DP, Wu J (2008) Fragmented QRS as a marker of conduction abnormality and a predictor of prognosis of Brugada syndrome. *Circulation* 118:1697–1704
 14. Papadatos GA, Wallerstein PM, Head CE, Ratcliff R, Brady PA, Benndorf K, Saumarez RC, Trezise AE, Huang CL, Vandenberg JJ, Colledge WH, Grace AA (2002) Slowed conduction and ventricular tachycardia after targeted disruption of the cardiac sodium channel gene Scn5a. *Proc Natl Acad Sci USA* 99:6210–6215
 15. Postema PG, van Dessel PF, Kors JA, Linnenbank AC, van Herpen G, Ritsema van Eck HJ, van Geloven N, de Bakker JM, Wilde AA, Tan HL (2010) Local depolarization abnormalities are the dominant pathophysiologic mechanism for type 1 electrocardiogram in brugada syndrome a study of electrocardiograms, vectorcardiograms, and body surface potential maps during ajmaline provocation. *J Am Coll Cardiol* 55:789–797
 16. Ractliffe JF (1967) *Elements of mathematical statistics*, 2nd edn. Oxford U.P, London
 17. Royer A, van Veen TA, Le Bouter S, Marionneau C, Griol-Charhbil V, Leoni AL, Steenman M, van Rijen HV, Demolombe S, Goddard CA, Richer C, Escoubet B, Jarry-Guichard T, Colledge WH, Gros D, de Bakker JM, Grace AA, Escande D, Charpentier F (2005) Mouse model of SCN5A-linked hereditary Lenegre's disease: age-related conduction slowing and myocardial fibrosis. *Circulation* 111:1738–1746
 18. Sacher F, Meregalli P, Veltmann C, Field ME, Solnon A, Bru P, Abbey S, Jais P, Tan HL, Wolpert C, Lande G, Bertault V, Derval N, Babuty D, Lacroix D, Boveda S, Maury P, Hocini M, Clementy J, Mabo P, Lemarec H, Mansourati J, Borggrefe M, Wilde A, Haissaguerre M, Probst V (2008) Are women with severely symptomatic brugada syndrome different from men? *J Cardiovasc Electrophysiol* 19:1181–1185
 19. Saumarez RC, Chojnowska L, Derksen R, Pytkowski M, Sterlinski M, Huang CL, Sadoul N, Hauer RN, Ruzylo W, Grace AA (2003) Sudden death in noncoronary heart disease is associated with delayed paced ventricular activation. *Circulation* 107:2595–2600
 20. Saumarez RC, Grace AA (2000) Paced ventricular electrogram fractionation and sudden death in hypertrophic cardiomyopathy and other non-coronary heart diseases. *Cardiovasc Res* 47:11–22
 21. Saumarez RC, Pytkowski M, Sterlinski M, Hauer RN, Derksen R, Lowe MD, Szwed H, Huang CL, Ward DE, Camm AJ, Grace AA (2006) Delayed paced ventricular activation in the long QT syndrome is associated with ventricular fibrillation. *Heart Rhythm* 3:771–778
 22. Shimizu W (2004) Gender difference and drug challenge in Brugada syndrome. *J Cardiovasc Electrophysiol* 15:70–71
 23. Stokoe KS, Balasubramaniam R, Goddard CA, Colledge WH, Grace AA, Huang CL (2007) Effects of flecainide and quinidine on arrhythmogenic properties of Scn5a+/- murine hearts modelling the Brugada syndrome. *J Physiol* 581:255–275
 24. Turner I, Huang CLH, Saumarez RC (2005) Numerical simulation of paced electrogram fractionation: relating clinical observations to changes in fibrosis and action potential duration. *J Cardiovasc Electrophysiol* 16:151–161
 25. van Veen TA, Stein M, Royer A, Le Quang K, Charpentier F, Colledge WH, Huang CL, Wilders R, Grace AA, Escande D, de Bakker JM, van Rijen HV (2005) Impaired impulse propagation in Scn5a-knockout mice: combined contribution of excitability, connexin expression, and tissue architecture in relation to aging. *Circulation* 112:1927–1935
 26. Yan GX, Antzelevitch C (1999) Cellular basis for the Brugada syndrome and other mechanisms of arrhythmogenesis associated with ST segment elevation. *Circulation* 100:1660–1666
 27. Zipes DP, Jalife J (2004) *Cardiac electrophysiology: from cell to bedside*, 4th edn. Saunders, Philadelphia